Sand Composition of The Gran Desierto: A Terrestrial Analogue for Thermal Infrared Imaging and Spectroscopy Techniques. S. P. Scheidt[1], N. Lancaster[1], and M. S. Ramsey[2], [1]Desert Reseearch Institute, 2215 Raggio Parkway, Reno, NV 89512, sscheidt77@gmail.com. [2]Department of Geology and Planetary Science, University of Pittsburgh, Pittsburgh, PA.

Introduction: The Gran Desierto in Sonora, Mexico, currently the largest active sand sea in North America, is an important aeolian depositional system wherein a number of possible local- to regional-scale sand transport pathways exist for sources of sand of varied composition. Dune morphology has been extensively studied to explain the history of the dune field [1,2,3,4]. The composition of sands in the Gran Desierto have been studied using geochemical and grain-size analysis at its margins [6] and in other regional aeolian deposits [e.g., 7,8]. These studies suggest that the sands of the Gran Desierto were sourced from the ancestral bed load of the Colorado River [9].

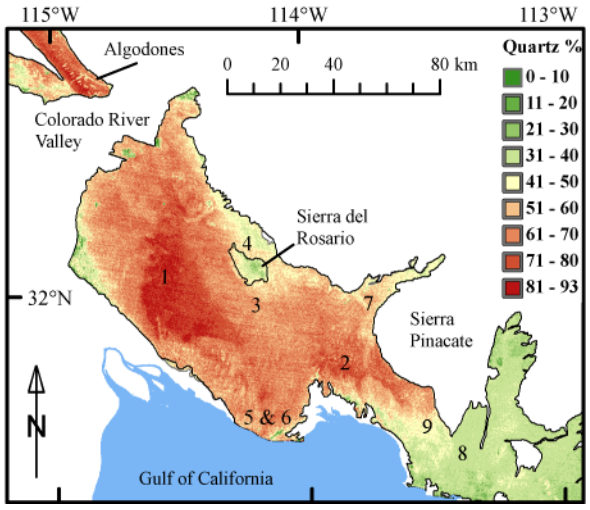

Figure 1. Map of the Gran Desierto dune field showing ASTER derived quartz abundance, which is comparable to the quartz/feldspar ratio. Numbers correspond to laboratory retrievals of different dune areas (see Table 1.)

Determination of surface mineral composition in previous studies of Desierto dunes [9] and other areas using reflectance data were limited due to the spectral complications of VNIR remote-sensing [e.g., 10]. In the thermal infrared (TIR) wavelength region however, mixing of emitted radiant energy is linearly related to the areal abundance of major dune forming minerals (e.g., silicates, carbonates and sulfates), which have diagnostic spectral absorption features [e.g., 11,12]. Linear deconvolution of TIR emission spectra from remote sensing and laboratory spectroscopy has been used as an effective tool for extracting the mineralogical composition of both Mars and Earth surface materials, including sand dunes [e.g., 13,14]. The Advanced Spaceborne Thermal Emission and Reflection Radiometer (ASTER) instrument has high spatial resolution (90m) and multispectral capabilities (5 bands) in the TIR wavelength region (8.125 - 11.65 µm) [15]. Detailed compositional mapping can be achieved using the full spectral capabilities of ASTER, where linear spectral deconvolution of ASTER TIR data alone have been accurate and quantitative [e.g., 16,17,18].

Geologic Setting: The majority of the dune field is located between the Colorado River Valley to the west; the Basin and Range Province to the north/northeast; and the shores of the Gulf of California to the south. East of the main dune field is the Sierra Pinacate volcanic complex, which is dominated by basalts. The center of the Gran Desierto overlies thick sequences of fluvial-deltaic sediments associated with the ancestral Colorado River.

There are several morphologic groups of dunes in the Gran Desierto which are hypothesized to be genetically different aeolian accumulations of different age and composition [1,2]. The major groups of dunes include a central core of star dunes, crescentic dunes that onlap the sand sheets and desert pavement to the west, linear dunes between the Sierra Pinacate and the Basin and Range, compound crescentic dunes north of the Bahia Del Adair, east and south of the Sierra Pinacate, and coastal parabolic and linear dunes to the southeast. Previously undescribed vegetated linear dunes are also distributed as far as 120 km southeast from the Sierra Pinacate along the coastal plain.

Approach: To accurately determine the spatial distribution of mineral composition (to within 3.1% [14]) of sand dunes in the Gran Desierto, this work describes a robust quantitative analysis of bulk mineralogy utilizing spectral deconvolution of both (1) a seamless, multispectral, radiometrically balanced mosaic of the ASTER TIR remote sensing data [18] and (2) high resolution thermal emission spectroscopy of aeolian sand samples using a Nicolet Nexus 670 spectrometer. Several field campaigns provided extensive coverage of surface (< 1 cm depth) sand samples, each representing a point measurement at the sub-pixel scale of the ASTER data. The spectra were acquired at a 2 cm^{-1} wavenumber spectral resolution between 2000

and 400 wavenumber (≈ 5-25 μm wavelength). A detailed description of the instrument and setup are found in [19]. The lab results were used for a detailed, systematic analysis of composition to select spectral end-members for ASTER data. The comparison of high resolution laboratory data to satellite data was critical to assessing accuracy of ASTER composition retrievals. Although of lower spectral resolution than laboratory data, the spatial continuity of mosaicked ASTER TIR data was critical to filling the gaps between the interpolations of field samples.

Results: Spectral end-members determined by laboratory analysis in decreasing order of average areal abundance are: quartz > plagioclase feldspar > potassium feldspar >> carbonate >> ferrohornblende. The interpolated laboratory data provide a moderate spatial resolution, hyperspectral TIR data cube from which the trends in bulk mineral abundance were revealed and comparable to ASTER retrievals of sand composition. Table 1 shows the bulk mineralogy lab results for different dune groups labeled in Figure 1.

Table 1. Normalized bulk mineralogy: quartz (Qt), total feldspar (Ft), plagioclase (Fn) and potassium feldspar (Fk). See Figure 1 for location references.

Region	Qt	Ft	Fn	Fk
(1) Central Dunes	78 ± 5%	22 ± 4%	22 ± 4%	--
(2) Eastern Crescentic	70 ± 4%	30 ± 5%	30 ± 6%	--
(3) Rosario (South)	59 ± 8%	41 ± 8%	38 ± 11%	3 ± 6%
(4) Rosario (North)	52 ± 8%	47 ± 10%	44 ± 13%	3 ± 6%
(5) Coastal (CO_3 rich)	59 ± 15%	41 ± 8%	36 ± 9%	5 ± 8%
(6) Coastal (Siliceous)	68 ± 5%	32 ± 3%	32 ± 3%	--
(7) Northern Pinacate	61 ± 11%	39 ± 11%	39 ± 8%	--
(8) Sonoyta Dunes	38 ± 7%	62 ± 6%	42 ± 12%	20 ± 16%
(9) Crescentic	56 ± 5%	44 ± 5%	34 ± 4%	10 ± 7%

Discussion: The laboratory and ASTER data results suggest that local feldspar-rich sources exert a much greater influence on sand composition than previously reported. The bulk of sand in the Gran Desierto can be described by a two sediment source mixing model between (a) quartz-rich Colorado River source material and (b) feldspar-rich local sources. Carbonate is a significant input for coastal sands. This sand composition model accounts for local feldspathic-rich sand input to dunes at the perimeter of the dune field, especially those close to the Sierra del Rosario and the Sonoyta River. These dunes have a high average feldspar abundance and closely resemble feldspar-rich aeolian sands from the Basin and Range in the Mojave Desert in their bulk composition (Ft > 40%) [7,8,14]. Variation in feldspar content also characterizes the Sonoyta Dunes, which have higher potassium feldspar content than other dunes in the sand sea. In the central portion of the dune field, a gradual compositional transition in the star dunes area can be seen in several remote-sensing datasets but is not detectable in the field. Our studies explained this transition as a gradational 30% increase in the quartz/feldspar ratio over a distance of 10 km from northeast to southwest across the star dune area. The high quartz/feldspar ratio in these dunes indicates a Colorado River sediment source (Qt > 75%) [7,8]. The highest quartz content (> 90%) was found in the western crescentic dunes. The eastern crescentic dunes averaged ~70% quartz.

Conclusions: The bulk mineralogy is characterized by: (1) quartz-rich Colorado River sediments and (2) feldspar-rich local sources. Feldspar-rich sources are similar to immature sands of the Mojave [7,8] supplied by the Basin and Range and the Sonoyta River, creating gradients of feldspar and quartz that reflect sediment transport pathways. These results suggest the importance of combining the advantages of hyperspectral point measurements and moderate resolution imager TIR data for Martian dune studies.

References: [1] Lancaster N. (1992), Sedimentology, 39, 631-644. [2] Lancaster N. (1995), Desert Aeolian Processes, pp. 11-35. [3] Beveridge C. et al. (2006), Sedimentology, 53, 1391-1409. [4] Ewing R. et al. (2007), Eos Trans. AGU, 88, abstract #NG41C-0673. [6] Kasper-Zubillaga J.J. et al. (2007), Earth. Surf. Proc. Land., 32, 489-508. [7] Muhs D. (2004), Geomorphology, 59, 247-269. [8] Zimbelman J.R. and Williams S.H. (2002), GSA Bull., 114, 490-496. [9] Blount G. et al. (1990), JGR, 95, 15463-15482. [10] Hapke B. (1981), JGR, 86, 3039-3054. [11] Thomson J.L. and Salisbury J.W. (1993), Rem. Sens. Environ., 45, 1-13. [12] Ramsey M.S. and Christensen P.R. (1998), JGR, 103, 577-596. [13] Bandfield J.L. et al (2002), JGR, 107, E11, 5092. [14] Ramsey M.S. et al. (1999), GSA Bull., 111, 646-662. [15] Yamaguchi Y. et al. (1998), IEEE T. Geosci. Remote., 36, 1062–1071. [16] Wright S.P. and Ramsey, M.S. (2006), JGR, 111(E8). [17] Katra I. et al. (2008), Geomorphology, 105(3-4), 277-290. [18] Scheidt et al. (2008), Rem. Sens. Environ., 112, 920-933. [19] Ruff et al. (1997), JGR, 102, 14899-14913.